Electron detachment from negative ions by few-cycle laser pulses: Dependence on pulse duration

Christian Arendt, Darko Dimitrovski,* and John S. Briggs
Theoretische Quantendynamik, Universität Freiburg, Hermann-Herder-Strasse 3, D-79104 Freiburg, Germany
(Received 11 May 2007; published 27 August 2007)

Electron detachment from negative ions by few-cycle laser pulses is considered. The results of a full numerical solution of the time-dependent Schrödinger equation are compared to those from several analytic approaches. A nonmonotonic dependence of the detachment probability on the pulse duration at small field amplitudes ($\ll 1$ a.u.) is observed and explained. In addition, momentum distributions of detached electrons are presented and analyzed.

DOI: 10.1103/PhysRevA.76.023423 PACS number(s): 32.80.Rm, 32.80.Gc, 32.80.Fb

I. INTRODUCTION

A decade has passed since the first experimental generation of few-cycle pulses in the near infrared (for a review, see [1]). Recently the techniques for experimental generation of such pulses have advanced and the electric field temporal shape can be controlled and known in full detail [2]. The first experiments with few-cycle pulses were concerned with the experimental proof of the influence of the relative phase of envelope and carrier [3] and this has been the subject of many other studies (for a recent review, see [4]). However, in this paper we will not consider carrier-envelope effects, rather we concentrate on the description of the nonmonotonic dependence of the ionization probability as a function of pulse duration, which has been observed in numerical studies [5–7]. We show that the origin of such behavior is the same as the "zigzag" dependence of the probability of detachment (ionization) reported in a previous paper [8] on half-cycle ionization of atomic systems. In contrast to the previous work, here few-cycle pulses are analyzed instead of half-cycle ones, the strong-field approximation [9,10] is used as an additional analytic tool and momentum distributions of detached electrons are presented and analyzed.

This paper is organized as follows. In the next section we present the problem and the numerical procedure used for its solution. In the third section the analytic approaches to be used in the analysis are introduced. These are first-order perturbation theory (FPA), the strong-field approximation (SFA), and the theory of the tunneling processes. Results for the total detachment probability as a function of pulse duration are presented and discussed in Sec. IV. In Sec. V we deal with the momentum distribution of detached electrons. Atomic units ($e=\hbar=m_e=1$) are used throughout.

II. THE PROBLEM AND ITS NUMERICAL SOLUTION

The detachment of the outer electron from negative ions by a linearly polarized laser field is described in dipole approximation by the time-dependent Schrödinger equation

$$i\frac{\partial\psi(\mathbf{r},t)}{\partial t}=\left(-\frac{1}{2}\Delta+V(\mathbf{r})+\mathbf{F}(t)\cdot\mathbf{r}\right)\psi(\mathbf{r},t), \tag{1}$$

where $\mathbf{F}(t)$ is the electric field of the laser and we have used a single-active-electron model of the negative ion. The corresponding one-electron initial state is an eigenstate of the Hamiltonian in Eq. (1) with V being the three-dimensional zero-range potential (ZRP)

$$V(\mathbf{r})=\frac{2\pi}{\alpha}\delta(\mathbf{r})\frac{\partial}{\partial r}r. \tag{2}$$

The ZRP potential [11] is much used in atomic physics, particularly for multiphoton detachment of electrons from negative ions (for a review, see [12]). Such a potential supports only one bound state with energy $E_0=-\alpha^2/2$ whose normalized wave function is

$$\psi_0(\mathbf{r})=\left(\frac{\alpha}{2\pi}\right)^{1/2}\frac{e^{-\alpha r}}{r}, \tag{3}$$

and the continuum wave functions corresponding to momentum $\mathbf{p}$ are

$$\psi_{\mathbf{p}}(\mathbf{r})=(2\pi)^{-3/2}\left(e^{i\mathbf{p}\cdot\mathbf{r}}-\frac{1}{\alpha+ip}\frac{e^{ipr}}{r}\right). \tag{4}$$

For the sake of definiteness, the electric field of the laser is assumed to have a Gaussian envelope

$$\mathbf{F}(t)=F_0\sin\left(\frac{n\pi t}{2\tau}\right)e^{-(t/\tau)^2}. \tag{5}$$

In the above equation τ is the pulse duration and n is the number of cycles of the field. In this study we present numerical solutions for pulses with $n\leqslant 2$.

The use of the ZRP admits a scaling of Eq. (1), by introducing the transformations $t'\rightarrow\alpha^2 t$, $r'\rightarrow\alpha r$. As a result of these transformations, the magnitude of the electric field of the pulse scales as $F'=F/\alpha^3$ and the pulse duration scales as $\tau'=\alpha^2\tau$, while the energy of the bound state remains fixed at $E_0'=-1/2$. The scaled equation reads

$$i\frac{\partial\psi(\mathbf{r}',t')}{\partial t'}=\left(-\frac{1}{2}\Delta_{\mathbf{r}'}+2\pi\delta(\mathbf{r}')\frac{\partial}{\partial r'}r'+\mathbf{F}'(t')\cdot\mathbf{r}'\right)\psi(\mathbf{r}',t'). \tag{6}$$

In the following, the scaled equation is used and the primes are omitted.

*darko@physik.uni-freiburg.de

The transformation of the time-dependent Schrödinger equation (6) to yield an integral equation suitable for numerical calculation proceeds exactly as in Ref. [8]. Nevertheless, for the sake of completeness, we summarize the procedure here.

First, Eq. (6) is rewritten [13] in the form of a Lippmann-Schwinger equation

$$\psi(\mathbf{r},t) = \int_{-\infty}^{t} dt' \int d^3\mathbf{r}' G(\mathbf{r},t;\mathbf{r}',t') V(\mathbf{r}')\psi(\mathbf{r}',t'), \quad (7)$$

where

$$G(\mathbf{r},t;\mathbf{r}',t') = G_0(\mathbf{r}-\mathbf{r}',t-t')e^{-i\mathcal{M}(t,t')}e^{-i\mathcal{R}(\mathbf{r},t;\mathbf{r}',t')} \quad (8)$$

is the Volkov's Green function and

$$G_0(\mathbf{r}-\mathbf{r}',t-t') = -i\theta(t-t')\frac{e^{i[(\mathbf{r}-\mathbf{r}')^2/2(t-t')]}}{[2\pi i(t-t')]^{3/2}} \quad (9)$$

is the Green function of the free particle. The functions $\mathcal{M}$ and $\mathcal{R}$ are defined as

$$\mathcal{M}(t,t') = \frac{1}{2}\left[\int_{t'}^{t} dt'' \mathbf{A}^2(t'') - \frac{1}{t-t'}\left(\int_{t'}^{t} dt'' \mathbf{A}(t'')\right)^2\right],$$
$$\mathcal{R}(\mathbf{r},t;\mathbf{r}',t') = -\left(\mathbf{A}(t)\cdot\mathbf{r} - \mathbf{A}(t')\cdot\mathbf{r}' - \frac{\mathbf{r}-\mathbf{r}'}{t-t'}\int_{t'}^{t} dt''\mathbf{A}(t'')\right). \quad (10)$$

In the above equations $\theta(t)$ is the Heaviside step function and $\mathbf{A} = -\int_{-\infty}^{t} dt' \mathbf{F}(t')$ is the vector potential.

Second, by defining the function

$$R(t) = -(2\pi)^{1/2} e^{-it/2} \lim_{r\to 0} \frac{\partial}{\partial r} r\psi(\mathbf{r},t), \quad (11)$$

and using the special properties of the ZRP potential, Eq. (7) for the wave function $\psi(\mathbf{r})$ is reduced to the following one-dimensional integral equation [13]:

$$R(t) = -(2\pi i)^{-1/2}\int_0^{\infty} \frac{dt'}{t'^{3/2}}[e^{-i\mathcal{M}(t,t-t')}e^{-it'/2}R(t-t') - R(t)]. \quad (12)$$

Having solved Eq. (12) one is able to reconstruct the wave function from $R(t)$ by performing the integration

$$\psi(\mathbf{r},t) = (2\pi)^{-1} i^{-1/2}\int_0^{\infty} \frac{dt'}{t'^{3/2}} e^{ir^2/2t'} e^{i(t-t')/2} e^{-i\mathcal{M}(t,t-t')} e^{-i\mathcal{R}(\mathbf{r},t,0,t-t')} R(t-t'). \quad (13)$$

When $R(t)$ is calculated, one can obtain the detachment probability by generating the wave function using Eq. (13), projecting it onto the continuum wave functions, and finally, integrating over final state momenta. Alternatively, one can obtain the detachment probability directly from $R(t)$ as

$$P = 1 - \lim_{t\to\infty} |R(t)|^2. \quad (14)$$

A formal proof of the above equation is given in Appendix A.

Generally the method of obtaining the detachment probability directly from $R(t)$ is faster. However, for small total detachment probability (usually smaller than 10^{-6}) it is imprecise, since the errors from the solution of the integral equation become of the same order as $1-R(t)$. In such cases the (slower) method of reconstruction of the total wave function $\psi(\mathbf{r},t)$ should be used. The details of the numerical procedure for the solution of the integral equation in $R(t)$ of Eq. (12) and the numerical reconstruction of $\psi(\mathbf{r},t)$ from $R(t)$ are given in [14].

III. ANALYTIC METHODS

In this section we present the analytic tools used. In the case of weak fields and short pulse duration we use first-order time-dependent perturbation theory (FPA). In the limit of large pulse duration τ an expression for the tunneling probability is used. In addition to the above approximations, valid in the special cases of short and long pulses, respectively, we use the strong-field approximation (SFA) [9,10] for all pulse durations and amplitudes and compare the results of the three approaches.

A. First-order perturbation theory

In first-order time-dependent perturbation theory the transition amplitude from the bound state ψ_0 to the continuum state $\psi_{\mathbf{p}}$ with momentum $\mathbf{p}$ is

$$a_{per}(\mathbf{p}) = -i\langle\psi_{\mathbf{p}}|z|\psi_0\rangle\int_{-\infty}^{\infty} F(t)\exp\left[i\frac{(p^2+\alpha^2)t}{2}\right]dt, \quad (15)$$

where, using the continuum wave function from Eq. (4) one obtains

$$\langle\psi_{\mathbf{p}}|z|\psi_0\rangle = \frac{2\sqrt{\alpha}p\cos\theta}{\pi(\alpha^2+p^2)^2}, \quad (16)$$

with θ the angle between $\mathbf{p}$ and $\mathbf{F}$. Then the total detachment probability is obtained as

$$P_{per} = \int |a_{per}(\mathbf{p})|^2 d^3\mathbf{p}. \quad (17)$$

B. Adiabatic approximation: Tunneling

In the adiabatic limit $\tau \to \infty$, the process of detachment is dominated by the tunneling mechanism. It has been shown that the expression for the tunneling probability is in fact the zeroth-order adiabatic result [15], that is, the probability of detachment can be written as

$$P_{tun} = 1 - \exp\left(2\ \mathrm{Im} \int_{-\infty}^{+\infty} E(F(t))dt\right)$$
$$= 1 - \exp\left(-\int_{-\infty}^{+\infty} \Gamma(F(t))dt\right). \tag{18}$$

In the above equation E is the complex-valued energy obtained as a solution of the stationary problem of an electron in a ZRP potential plus constant electric field in the quasistationary state approach [16–18]. In the limit $F \to 0$, the quasistationary state goes over into the bound state of the ZRP (3) and the energy E goes over into the bound state energy E_0. This *complex* energy can be written as

$$E(F) = E_0 + \Delta E(F) - i\frac{\Gamma(F)}{2}, \tag{19}$$

where E_0 is the bound state eigenenergy in the absence of the electric field, ΔE is the Stark shift of the energy level, and Γ is its width. To calculate the tunneling probability (18) this width of the bound state is needed. In the case of weak fields, a simple analytic expression is available [19] as follows:

$$\Gamma(F) = \frac{F}{2\alpha}\exp\left(-\frac{2\alpha^3}{3F}\right). \tag{20}$$

In cases when the field is not weak, one has to solve the eigenvalue equation numerically in the quasistationary state approach to obtain $\Gamma(F)$. This procedure results in the following transcendental equation [20]:

$$\pi a[b\mathrm{Ai}(b)\mathrm{Ci}(b) - \mathrm{Ai}'(b)\mathrm{Ci}'(b)] = \alpha, \tag{21}$$

where

$$\mathrm{Ci}(b) = \mathrm{Bi}(b) + i\mathrm{Ai}(b), \tag{22}$$

and Ai and Bi are two independent solutions of the Airy equation, with $a=(2F)^{1/3}$ and $b=-2E(F)/a^2$. By solving numerically Eq. (21) the complex function $E(F)$ is obtained. The expression for $\Gamma(F)$ of Eq. (20) can be obtained as the asymptotic solution of the transcendental Eq. (21) in the limit $F \to 0$. For weak fields the expression (20) and the numerical solution of Eq. (21) give the same result. For all other field strengths $\Gamma(F)$ of Eq. (20) is larger than the numerically calculated $\Gamma(F)$ from Eq. (21). Therefore, when substituted in the equation for the tunneling probability (18), $\Gamma(F)$ of Eq. (20) will overestimate the detachment probability for these field strengths.

C. Strong-field approximation

The Keldysh approach or the strong-field approximation (SFA) was originally developed for laser fields consisting of an infinite number of cycles [9,10]. In the last decade this approach has been used to analyze ionization of atomic systems by few-cycle laser pulses (see, for example [4], and references therein). The transition amplitude from the ground state to the continuum state of momentum $\mathbf{p}$ in the formalism of SFA is

$$a_{SFA}(\mathbf{p}) = -i\int_{-\infty}^{\infty} dt\langle \mathbf{p} + \mathbf{A}(t) - \mathbf{A}(\infty)|\mathbf{F}(t)\cdot\mathbf{r}|\psi_0\rangle \exp[iS(t)], \tag{23}$$

where

$$\langle \mathbf{p} + \mathbf{A}(t) - \mathbf{A}(\infty)|\mathbf{r}\rangle = \frac{1}{(2\pi)^{3/2}}\exp\{-i[\mathbf{p} + \mathbf{A}(t) - \mathbf{A}(\infty)]\cdot\mathbf{r}\} \tag{24}$$

is a plane wave and $\mathbf{A}(t) = -\int_{-\infty}^{t} dt'\mathbf{F}(t')$ is the vector potential of the laser field. The phase $S(t)$ that appears in Eq. (23) is given by

$$S(t) = -\int_{-\infty}^{t} dt'[E_i - E_f(t')], \tag{25}$$

where E_i is the energy of the initial state and E_f is the instantaneous energy of the final state, given by

$$E_i = E_0 = -\frac{\alpha^2}{2}, \tag{26}$$

and

$$E_f(t') = \frac{1}{2}[\mathbf{p} + \mathbf{A}(t') - \mathbf{A}(\infty)]^2. \tag{27}$$

The appearance of the final vector potential $\mathbf{A}(\infty)$ in Eq. (23) enables one to include in the analysis the cases of nonzero value of the vector potential at the end of the pulse [21]. Namely, with the correction $\mathbf{A}(\infty)$, the Volkov state goes over into the usual plane wave when the interaction with the field is over (i.e., for $t \to \infty$), as should be.

For all pulse amplitudes F_0 and pulse durations τ the transition amplitude in SFA (23) can be calculated numerically. In the case of large pulse duration, the phase $S(t)$ becomes large and it is possible to perform the integral in Eq. (23) analytically using the modification of the saddle-point method proposed in Ref. [22]. We have checked that the analytical integration and numerical calculation of the transition amplitude (23) in the case of large τ yield the same result.

The transition amplitude of Eq. (23) differs from the usual time-dependent perturbation theory in that Volkov states are taken as final states rather than undistorted plane waves [9]. Therefore one expects that such an approach will, in general, be valid only in cases where the initial state is not depleted appreciably. On the other hand, in the adiabatic limit $\tau \to \infty$, the Volkov final state plays the role of the approximate adiabatic final state and $\exp[-iS(t)]$ of Eq. (23) is the correct adiabatic exponent [16]. In general, the influence of the atomic potential in SFA is taken into account only through the dipole matrix element from the initial state to the continuum. That is, once the electron reaches the continuum it is

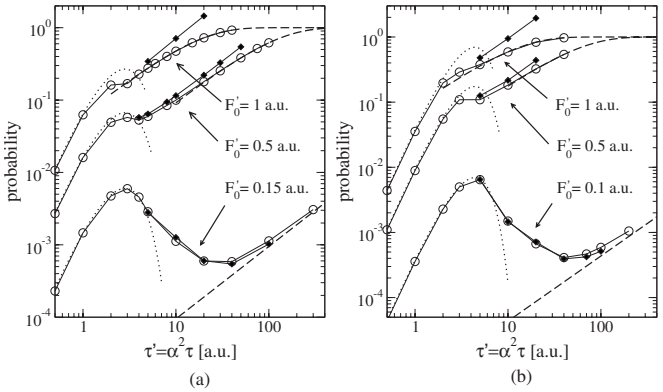

FIG. 1. Numerical results for the detachment probability by (a) one-cycle and (b) two-cycle pulses (open circles) as a function of pulse duration compared to first-order perturbation theory (dotted line), tunneling probability (dashed line) and the strong-field approximation (black diamonds).

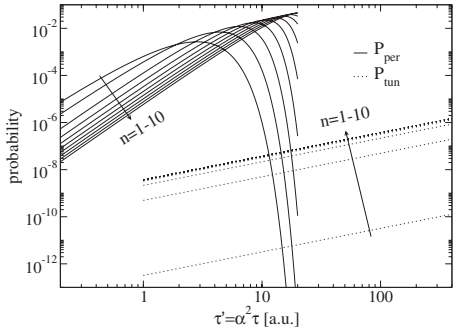

FIG. 2. Short-time and adiabatic asymptotes for $n=1-10$ cycle pulses, defined in Eq. (5), and for pulse amplitude $F_0/\alpha^3=0.05$. Full lines depict the first-order perturbation theory (short-time asymptotes) and the dotted lines depict the tunneling probability (adiabatic asymptotes). The arrows show the direction in which the asymptotes move as the number of cycles increase from $n=1$ to $n=10$.

treated as a free particle, which moves in the electric field of the laser. This makes the case of the ZRP ideal for the application of the SFA, since the influence of this potential on the free particle can be neglected to very good approximation. This is in contrast to the case of, e.g., a Coulomb potential with its infinite range, which influences the dynamics of the laser-driven electron in the continuum.

IV. TOTAL DETACHMENT PROBABILITY

Results of numerical calculations for the total detachment probability for a one-cycle pulse [the pulse from Eq. (5) with $n=1$] as a function of pulse duration τ are given in Fig. 1(a). The various curves correspond to different pulse amplitudes F_0/α^3. Essentially the behavior of the detachment probability is very similar to the case of half-cycle ionization reported in Ref. [8].

Before we proceed with the analysis using the scaled units of field strength $F_0'=F_0/\alpha^3$ and pulse duration $\tau'=\alpha^2\tau$, it is useful to get some idea about the actual numbers by considering the example of the negative ion of hydrogen H^-. The binding energy of H^- is 0.754 eV ($|E_0|=2.77\times10^{-2}$ a.u.) and therefore the scaling parameter $\alpha=\sqrt{2|E_0|}=0.235$. In this case a scaled field strength of, for example, $F_0'=0.1$ corresponds to a field strength of $F_0=1.3\times10^{-3}$ a.u. (equivalent peak laser intensity of 5.93×10^{10} W/cm^2) and a scaled pulse duration of $\tau'=1$ corresponds to a pulse duration of $\tau=18$ a.u. (0.435 fs).

For strong fields the detachment probability increases monotonically with the pulse duration at constant pulse amplitude, an intuitive result. However, for weak fields ($F_0'=F_0/\alpha^3\ll1$) after the initial rise for very short pulses, the detachment probability exhibits a maximum and decreases before it restores the monotonic rise for large pulse durations. This behavior of the detachment probability as a function of pulse duration arises, as we will see below, from a transition between the perturbative and the tunneling regimes.

The case of one cycle is not special. The same behavior persists when one changes the number of cycles. As an example, the one-cycle and two-cycle cases are compared in Fig. 1. There is hardly any qualitative difference in the behavior of the curves. On the same figure various approximations, defined in Sec. III, are compared to the numerical results.

In the case of short pulses, the numerical results can be reproduced within the FPA of Eqs. (15)–(17) up to $\tau'=\alpha^2\tau\sim3$. For smaller pulse amplitudes, the FPA agrees with the numerical results up to larger pulse durations. With an increase of the pulse amplitude the agreement of FPA and numerical results breaks down at smaller and smaller pulse durations. The maximum in the numerical results for weak fields is reproduced nicely within the FPA and is independent of pulse amplitude. In the case of a one-cycle pulse the maximum is at $\alpha^2\tau\approx2.84$ and for the two-cycle case the maximum is positioned at $\alpha^2\tau\approx4.41$ (see Fig. 2 as well). As the number of cycles increases the maximum moves in the direction of higher τ's. In the case of strong fields the FPA breaks down before its maximum and the numerical results rise monotonically as a function of the pulse duration.

In the opposite (adiabatic) limit of pulses with large τ the tunneling mechanism dominates. However, in contrast to the case of a half-cycle pulse, the expression (18) is not directly applicable here since the electric field of the pulse performs oscillations. Assuming that in each half cycle of the field a certain population tunnels out from the potential and that this electron *never* recombines with its parent atom, it is possible to use the tunneling formula (18) with $F(t)$ replaced by its absolute value $|F(t)|$. In the case of a Coulomb potential such an assumption is shown to be justified at field strengths, which suppress the Coulomb barrier below the energy of the initial state (in the regime of above-barrier ionization) [23]. The result of a calculation using $|F(t)|$, shown in Fig. 1 for both one- and two-cycle cases, confirms that the above assumption is valid. Namely, the tunneling expression correctly reproduces the numerical results for large τ's and for all pulse amplitudes. The rescattering process might have an influence on the detached electron momentum distribution [4], but, in the case considered here, it has negligible contribution to the total detachment probability.

The tunneling probability and the FPA act as asymptotes of the numerically calculated detachment probability as can

be seen in Fig. 1. However, their dependence on the pulse amplitude F_0 is different. Whilst the FPA is proportional to F_0^2, the tunneling expression in the case of weak fields (20) has an exponential dependence on F_0 and therefore the tunneling (adiabatic) asymptote decreases (as a function of pulse amplitude F_0' at a fixed pulse duration τ) much faster than the short-time asymptote described by the FPA. The relative positions of the asymptotes decide the nonmonotonic dependence. For strong fields ($F_0' \sim 1$ a.u.), the relative position of the short-time and the adiabatic asymptote is such that the detachment probability curve makes a transition from one asymptote to the other, keeping the monotonic rise. On the other hand, for weak fields ($F_0' \ll 1$ a.u.), the tunneling curve lies several orders of magnitude under the perturbation curve and therefore the total detachment probability exhibits a local maximum and decreases before increasing again to "lock" to the tunneling asymptote—a "zigzag" effect [8]. This effect is more pronounced the smaller is the field amplitude (see Fig. 1).

The above effect of nonmonotonic dependence on pulse duration should persist for more than two cycles, though with the increase of the number of cycles the nonmonotonic dependence is ironed out. This can be seen in Fig. 2 where the relative position of short-time and adiabatic asymptotes is depicted as a function of pulse duration and number of cycles of the pulse. A particular pulse amplitude $F_0/\alpha^3 = 0.05$ is taken, where the drop in the detachment probability going from the perturbative to the tunneling regime is substantial for a one-cycle pulse. As the number of cycles n increases, the short-time (FPA) asymptote moves toward lower probabilities. On the other hand the adiabatic (tunneling) asymptote rises as the number of cycles increases. The change in position of the asymptotes is larger the smaller the number of cycles. At the particular pulse amplitude of Fig. 2, after a large displacement in transition from single to few cycles, the tunneling asymptote hardly moves after n exceeds four. The overall result of the increase of the number of cycles is that the adiabatic and tunneling asymptote approach each other. Whether the increase of the number of cycles results in the complete disappearance of the zigzag effect or not depends on the following factors. First, it depends on the pulse amplitude F_0—at larger pulse amplitudes the likelihood of ironing out the effect is greater. Secondly, it depends at which pulse duration τ does the validity of the first-order perturbation cease and at which τ the validity of the tunneling expression begins, as the number of cycles increases. These pulse durations for an arbitrary number of cycles can be determined by performing full numerical calculation for the specific cases.

The experimental reproduction of the drop in the detachment probability as a function of the pulse duration, shown in Figs. 1 and 2, is within reach. Taking negative hydrogen ion as a representative example, the requirement to observe the drop in the detachment probability is that the electric field amplitude is less than 1.3×10^{-3} a.u., which is equivalent to the requirement that the peak intensity of the laser is smaller than 5.93×10^{10} W/cm^2. In addition, one must be able to produce few-cycle pulses with the duration of $\tau' \sim 5$ to $\tau' \sim 50$, which in turn converts to the range from 2.2 to 22 fs and in terms of full width at half maximum (FWHM) of the pulse envelope the interval from 3.6 to 36 fs. Truly few-cycle pulses with FWHM in the above range have been already generated experimentally (see, e.g., [1–3]), albeit at larger intensities than those required to observe the nonmonotonic dependence analyzed here. Therefore the production of short few-cycle pulses with lower intensities should be currently feasible.

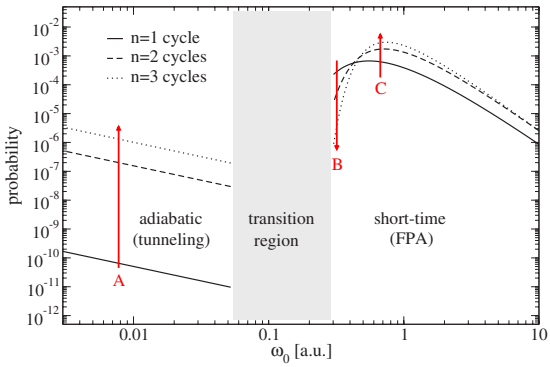

FIG. 3. (Color online) Detachment probability as a function of pulse frequency $\omega_0 = n\pi/(2\alpha^2\tau)$ for $n = 1, 2, 3$ cycle pulses and for pulse amplitude $F_0/\alpha^3 = 0.05$. Both short-time (FPA) and adiabatic (tunneling) asymptotes are given. The red arrows indicate what happens when the pulse length increases at a fixed frequency. See the text for other details.

As mentioned in the Introduction, the nonmonotonic dependence of ionization probability on pulse duration in Fig. 1 is already observed in numerical studies [5–7]. The fall of the ionization probability as a function of pulse duration occurs for weak fields and for pulse durations of the order of one cycle. However, in contrast to our study where the shape of the pulse is not changed with the pulse duration, in Refs. [5–7] the pulse duration is increased by increasing the cycle number and keeping the frequency constant. Another point is that in the studies [5,6] the hydrogen atom is analyzed whereas in [7] ionization of a single active electron in sodium is considered. Although in the above studies different atomic systems are used, and pulses with a $\sin^2$ envelope are considered [5,6], here we show that the explanation of the fall of ionization probability as a function of pulse duration can be given by simply looking at the model of the zero-range potential, where there are no excited states, and considering the relative position of the adiabatic and short-time asymptote without making any explicit numerical calculations.

The drop in ionization probability was discussed in detail in [5] (and the authors in [6] suggest they have reproduced this drop), so we will compare directly to these previous results. It is clear that in such a comparison one cannot expect that the effects seen for hydrogen will occur at exactly the same frequencies as for the ZRP model. However, by choosing $\alpha = 1$ one can, at least, equate the binding energy in both cases and ensure that the drop occurs at similar frequencies in both cases.

To facilitate the comparison, in Fig. 3 we have plotted the short-pulse and adiabatic asymptotes as a function of pulse frequency $\omega_0 = n\pi/(2\alpha^2\tau)$. Different curves correspond to different cycle numbers of the field. The short-time (pertur-

bative) curve is plotted up to the frequencies at which it is expected that the exact results will match (right after the maximum). As in Fig. 2, a field strength of $F_0/\alpha^3=0.05$ has been chosen because at such field strengths the zigzag effect is well pronounced and detachment probabilities are comparable to the ionization probabilities in Fig. 3 in Ref. [5]. In Fig. 3 the arrows indicate in which direction the detachment probability changes as the number of cycles is increased from one to three at a fixed pulse frequency ω_0.

In the adiabatic regime, detachment rises as the pulse duration is increased (case A in Fig. 3). The same happens in the short-time region (case C in Fig. 3). However, at the border of validity of the first-order perturbation theory and the transition region (in which exact numerical calculation or the SFA approximation is needed to predict the detachment probability) there exists a region of frequencies where increasing the pulse duration results in a decrease in detachment probability by three orders of magnitude (case B in Fig. 3). In the case depicted in Fig. 3 (frequencies around 0.3 a.u.), upon increasing the number of cycles beginning from one cycle, the detachment probability will drop by a few orders of magnitude. In Fig. 3 of [5] the drop was detected for a frequency of 0.18 a.u. When the frequency is tripled to 0.55 a.u. (see Fig. 3 in Ref. [5]), the decrease is not observed. Instead, the ionization probability increases with the pulse length. Similarly, by tripling the frequency of $\omega_0=0.3$ a.u. (case B in Fig. 3) to $\omega_0=0.9$ a.u. (case C on the same figure) the drop in detachment probability transforms into an increase. Note that the existence of a decrease of detachment probability is not exclusive to the field amplitude depicted in Fig. 3—smaller field amplitudes will result in a larger drop.

Turning back to Fig. 1, the full curve with black diamonds plotted is the SFA of Eq. (23). As already pointed out in the previous section, the case of detachment of electrons from negative ions modeled by a ZRP is ideally suited for SFA application since, once the electron is in the continuum, the influence of the binding potential can be neglected. For weak fields, the SFA agrees excellently with the numerical results, not only in the extreme regions of short and long pulses, but also in the transition region. Specifically, the fall of the detachment probability for weak fields is reproduced excellently. These are natural consequences of the fact that the SFA amplitude (23) successfully combines both the perturbative and the tunneling mechanism.

However, for strong fields the SFA *overestimates* the detachment probability. Such a situation is depicted in detail in Fig. 4. In the case of a Coulomb potential, for pulse amplitudes that suppress the barrier, the SFA amplitude does not give the correct result for very strong fields [24]. In fact the issue of finding the appropriate ionization rate at above-barrier intensities has been the subject of many papers (see, e.g., [25–27]). However, in the case of detachment of negative ions modeled by a ZRP, the barrier exists *always*, no matter what the field strength. The comparison with our numerical calculation for one- and two-cycle pulses shows that once the total detachment probability exceeds ~0.1, or equivalently, once the initial state becomes appreciably depleted, the SFA breaks down.

The excellent agreement of numerical results with the tunneling probability, obtained in the quasistationary state approach, suggests that the same procedure can be applied to the case of the Coulomb potential in the barrier-suppression regime. The following evidence backs up such an assumption. In the case of half-cycle ionization of hydrogen there is an excellent agreement of the tunneling probability expression (18), where the width of the state Γ is obtained in the quasistationary state approach, with the *ab initio* results at field amplitudes that suppress the Coulomb barrier (see the curve for $F_0=0.1$ in Fig. 1(b) in Ref. [8]). Since in the barrier suppression regime recombination of electrons already in continuum with their parent atom or ion is unlikely, that is, at these field strengths the ionization from each half cycle can be treated independently, the tunneling probability expression will reproduce the numerical results very accurately in the case of few-cycle pulses as well. The decay width Γ of the initial state for the Coulomb potential as a function of field amplitude F can be obtained by the quasistationary state approach [28] or, alternatively, using the complex scaling method [26].

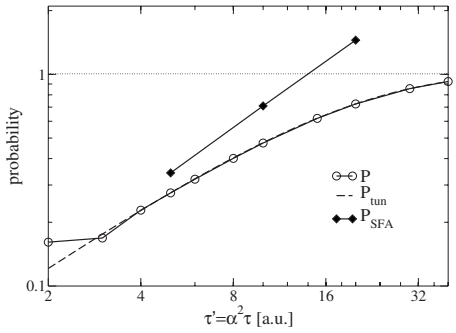

FIG. 4. Detachment probability as a function of pulse duration for one-cycle pulse and for pulse amplitude $F_0/\alpha^3=1$. Numerical results are compared to the tunneling probability and the strong-field approximation.

V. MOMENTUM DISTRIBUTIONS OF DETACHED ELECTRONS

The momentum distributions of detached electrons contain signatures of the dominant mechanisms operating in different regions of pulse duration. Here we restrict ourselves to analysis of momentum distributions resulting from one cycle in the weak-field limit ($F_0' \ll 1$ a.u.), where a nonmonotonic dependence of the detachment probability on pulse duration appears.

For short pulses the perturbative mechanism dominates. An example of such a situation is depicted in Fig. 5(a). The numerically calculated momentum distribution possesses p-type symmetry and can be reproduced both with the FPA and the SFA. Such a symmetry is a signature of the perturbative mechanism.

Upon increasing the pulse duration, the calculated momentum distribution becomes asymmetric with respect to the origin $p=0$. In Fig. 5(b) the case of $F_0/\alpha^3=0.1$ and $\tau\alpha^2=10$ is depicted. These parameters correspond to the region where the detachment probability decreases as a function of pulse duration. On the same figure, the numerical result is

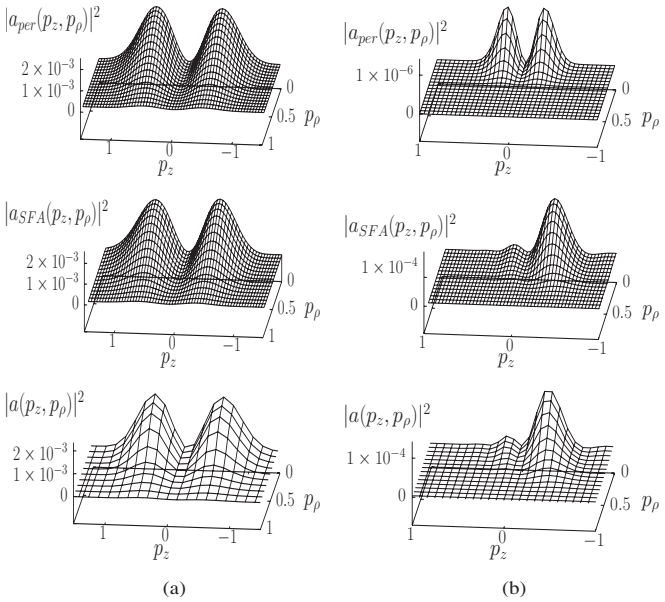

FIG. 5. Momentum distributions in a.u. of detached electrons by a one-cycle pulse with $F_0/\alpha^3=0.1$ and $\tau\alpha^2=3$ (a), and $F_0/\alpha^3=0.1$ and $\tau\alpha^2=10$. First row: first-order time-dependent perturbation theory; second row: strong-field approximation; third row: numerical results.

compared to the FPA and SFA. While the SFA reproduces the numerical result excellently, the FPA gives a result which is orders of magnitude smaller and with a p-type symmetry. We have checked numerically that by gradually increasing the pulse duration the absolute value of the momentum distribution is decreased and the peak at positive momenta is suppressed.

In the limit of long pulses interference in the continuum begins to play a role. Namely, the wave packet that tunnels out after a half cycle of the field interferes with the one which tunnels out in the subsequent cycle. As a result, one obtains momentum distributions of the type shown in Figs. 6(a) and 6(b). The larger is τ, the more will oscillations appear in the momentum distribution. These results confirm the results of Ref. [21] where such interference structures in the electron spectrum have been analyzed, however, only in the formalism of the SFA. Here we have given numerical confirmation of this effect. The interference structure can be shown in the corresponding energy distribution plotted in Fig. 6(c). The peaks in the energy distribution are a result of the interference of the population between the two half cycles and are not equidistant as are the above-threshold ionization peaks.

The occurrence of oscillations in the spectrum of detached electrons can be explained under the assumption that the detachment of the electrons occurs at the maximum of the field and that once the electron reaches the continuum, it does not recombine with its parent atom. Then the first half cycle puts the population in the continuum centered approximately around a momentum $A(0)/2$. The second half cycle changes the momentum of the electron wave packet in the continuum by an amount of $A(\infty)-A(0)$, so that the part of the momentum distribution that stems from the first half-cycle detachment will be centered approximately around $-A(0)/2$ after the second half cycle. However, this is precisely the mean momentum where the population that becomes detached by the second half cycle is centered. Hence the two contributions to the momentum distribution interfere strongly and the phase difference between these two contributions results in the interference pattern shown in Fig. 6.

The difference between the phases of the wave packets stemming from the different half cycles has been explained also in the formalism of SFA in Ref. [21] by splitting the SFA transition amplitude of Eq. (23) into two parts, each of which corresponds to different half cycles. Here we show that for large pulse durations the difference between the phases of the two electronic wave packets in the continuum can be calculated by applying the saddle-point method for the calculation of the SFA transition amplitude (23). The result of such a calculation (detailed in Appendix B) yields the transition amplitude

$$a_{SFA}(\mathbf{p}) = i\left(\frac{\alpha}{2\pi}\right)^{1/2} \frac{\exp\left(-i\int_{-\infty}^{t_s^{(1)}} dt[E_i - E_f(t)]\right)}{(\alpha^2+p_\rho^2)^{1/4}(F(t_s^{(1)}))^{1/2}} \times\left[1-\frac{\exp[i(\varphi_2-\varphi_1)]}{\exp[-i\arg F(t_s^{(1)})]}\right]. \tag{28}$$

In the above equation the phases φ_1 and φ_2 are defined as

$$\varphi_2 = -E_i(\mathrm{Re}\, t_s^{(2)} - \mathrm{Re}\, t_s^{(1)}),$$
$$\varphi_1 = -\int_{t_s^{(1)}}^{t_s^{(2)}} dt E_f(t), \tag{29}$$

where $t_s^{(1)}$ and $t_s^{(2)}$ are the saddle points corresponding to the electron detachment from the first and the second half cycle,

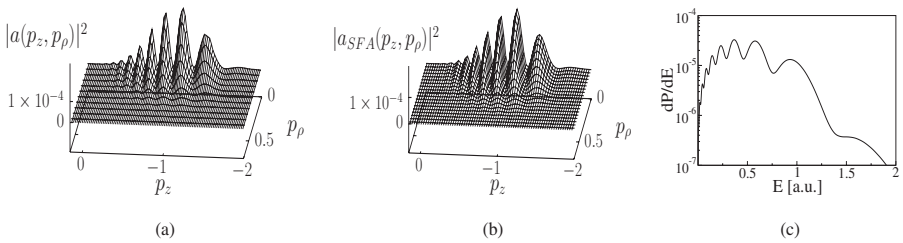

FIG. 6. Momentum distributions in a.u. of detached electrons by a one-cycle pulse for $F_0/\alpha^3=0.1$ and $\tau\alpha^2=30$. The results of a numerical calculation (a) are compared to the strong-field approximation result (b). The corresponding energy distribution is plotted in (c).

respectively, and their real part has the meaning of electron emission time. By calculating the SFA amplitude according to Eqs. (28) and (29) it is possible to obtain the momentum distribution given in Fig. 6, which shows interference between the electron wave packets originating from the two half cycles of a one-cycle pulse. The exponent involving the argument of the field at the saddle point $F(t_s^{(1)})$ is a weak function of $\mathbf{p}$ and its mean value is equal to π. Therefore the oscillations in momentum distribution arise mainly due to the phase difference $\varphi_2-\varphi_1$. The phase φ_2 of Eq. (29) is the energy phase acquired by the population that tunnels out in the second half cycle. On the other hand, the phase φ_1 is related to the electron wave packet that has tunneled out in the first half cycle.

VI. DISCUSSION AND CONCLUSIONS

We have analyzed detachment of electrons from negative ions by few-cycle pulses. The occurrence of a nonmonotonic dependence of detachment probability on pulse duration, previously encountered in several studies [5–7], is analyzed in full detail and explained theoretically. The origin of this effect is the same for half-cycle and few-cycle pulses. It is the transition between the perturbative and tunneling mechanism that results in a nonmonotonic dependence on pulse duration. Such an effect is not confined only to the zero-range potential. Analogous to the previous half-cycle results [8], the same qualitative dependence on pulse duration applies to the hydrogen atom as well. One should emphasize also that the envelope of the pulse is chosen to be Gaussian only for the sake of convenience; other pulse envelopes will produce a similar effect.

The nonmonotonic dependence on pulse duration is reproduced excellently by the strong-field approximation for weak and intermediate field strengths. However, for strong fields, where the depletion of the initial state is not negligible, the strong-field approximation overestimates the exact (numerical) result. The cause for such overestimation is the nonnegligible depopulation of the initial state.

Finally, the momentum distributions of the detached electron for different pulse durations have been analyzed. The transition from a symmetric to an asymmetric momentum distribution as the pulse duration increases has been illustrated. The symmetric momentum distribution is a signature of the perturbative mechanism. By contrast, in the adiabatic limit the interference of the wave packets of detached electrons originating from different half cycles gives rise to an oscillating structure. The oscillations can be explained as the energy phase difference between the wave packets originating from different half cycles.

ACKNOWLEDGMENTS

The support of the Deutsche Forschungsgemeinschaft through the project No. BR 728/13-1 is acknowledged gratefully.

APPENDIX A

Here we give a proof of Eq. (14) of Sec. II. Equation (14) is defined by the limit of infinite time. For finite times $\psi(\mathbf{r},t)$ can be written as

$$\psi(\mathbf{r},t) = C_0(t)\psi_0(\mathbf{r})e^{-iE_0t} + \int C_{\mathbf{p}}(t)\psi_{\mathbf{p}}(\mathbf{r})e^{-i(p^2/2)t}d^3\mathbf{p}. \tag{A1}$$

Therefore $R(t)$ of Eq. (11) contains contributions from both the bound state and from the spherical wave part of the continuum wave functions $\psi_{\mathbf{p}}$. As the pulse is turned off, the spherical wave leaves the origin, whereas the part of the wave function corresponding to the ground state stays. Specifically, the contribution of the spherical wave in $R(t)$ eventually vanishes. The formal proof of this assertion is as follows. In the limit $t\to\infty$, interaction with the pulse is over and the coefficients C_0 and $C_{\mathbf{p}}$ cease to be functions of time. Using the saddle-point method the integral in Eq. (A1) (the part of the wave function belonging to the detached electron) can be evaluated approximately as

$$\lim_{t\to\infty}\int C_{\mathbf{p}}\psi_{\mathbf{p}}(\mathbf{r})e^{-i(p^2/2)t}d^3\mathbf{p} \approx \sqrt{\frac{2\pi}{it^3}}\psi_{\mathbf{p}_0}(\mathbf{r})e^{-i(\mathbf{p}_0^2/2)t}, \tag{A2}$$

where $\mathbf{p}_0$ is the saddle point. Putting the above result into Eq. (A1) and using the definition (11) of $R(t)$ we obtain the result

$$\lim_{t\to\infty} R(t) = C_0 + \mathcal{O}(t^{-3/2}). \tag{A3}$$

From the above equation, it is evident that $R(t)$ in the limit of infinite times contains contribution only from the ground state because the spherical wave contribution falls off with time as $t^{-3/2}$. Therefore $\lim_{t\to\infty}|R(t)|^2$ has the meaning of the ground state occupation probability, so that Eq. (14) holds.

APPENDIX B

In this appendix we obtain the SFA amplitude in Eqs. (28) and (29) from Eq. (23) using a saddle-point analysis.

For sufficiently large pulse duration τ the phase in Eq. (23) becomes large, so the transition amplitude can be obtained by saddle-point integration. The dipole matrix element appearing in Eq. (23) is explicitly

$$\langle \mathbf{p}+\mathbf{A}(t)-\mathbf{A}(\infty)|\mathbf{F}(t)\cdot\mathbf{r}|\phi_0\rangle = \frac{\alpha^{1/2}}{2\pi}\frac{F(t)[p_z+A(t)-A(\infty)]}{\left\{\frac{1}{2}(\alpha^2+p_\rho{}^2+[p_z+A(t)-A(\infty)]^2)\right\}^2}. \tag{B1}$$

The saddle-point equation for each final momentum $\mathbf{p}$ of the electron reads

$$\alpha^2+p_\rho{}^2+[p_z+A(t_s^{(j)})-A(\infty)]^2=0, \quad j=1,\ldots,N, \tag{B2}$$

where $t_s^{(j)}=t_s^{(j)}(p_\rho,p_z)$ denotes the saddle point in the jth half cycle out of a total of N cycles. Further, p_z and p_ρ are the z and ρ component of the final momentum of the electron in the continuum. Actually, the saddle-point equation, in general has many pairs of complex-conjugate roots $t_s^{(j)}$, each pair corresponding to one half cycle in the few-cycle case. The

physically acceptable saddle points have positive imaginary parts ($\mathrm{Im}\, t_s^{(j)} > 0$) since their complex conjugates produce exponentially divergent momentum distributions. The real part of the saddle points is connected to the moment of the electron emission and the imaginary part is a measure of the inverse of the tunneling width Γ.

Comparing Eqs. (B1) and (B2), it is clear that the saddle points $t_s^{(j)}$ are also the poles of the dipole matrix element. Therefore the standard saddle-point method of integration does not apply. However, by using a modification of the saddle-point method [22] suitable for the cases of integrands having poles at the saddle point, the transition amplitude can be calculated as

$$a_{SFA}(\mathbf{p}) = i\left(\frac{\alpha}{2\pi}\right)^{1/2} \sum_{j=1}^{N} \frac{\exp[iS(t_s^{(j)})]}{[iS''(t_s^{(j)})]^{1/2}}, \tag{B3}$$

where

$$S''(t_s^{(j)}) = -F(t_s^{(j)})[p_z + A(t_s^{(j)}) - A(\infty)]. \tag{B4}$$

We consider the case of a one-cycle pulse, where there are only two terms in Eq. (B3) and relevant saddle points $t_s^{(1)}$ (first half cycle) and $t_s^{(2)}$ (second half cycle). For the pulses considered in this work [see Eq. (5)] the electric field is an odd function of time and therefore the relation satisfied by the field and the vector potential is

$$iF(t_s^{(1)}) = [iF(t_s^{(2)})]^* \quad \text{and} \quad A(t_s^{(1)}) = [A(t_s^{(2)})]^*. \tag{B5}$$

Because of the field symmetry (B5), the two saddle points corresponding to the same final electron momentum $\mathbf{p}$ satisfy the following relations:

$$\mathrm{Re}\, t_s^{(1)} = -\mathrm{Re}\, t_s^{(2)} \quad \text{and} \quad \mathrm{Im}\, t_s^{(1)} = \mathrm{Im}\, t_s^{(2)}. \tag{B6}$$

With the help of the saddle-point equation (B2), the SFA amplitude of Eq. (B3) transforms into Eq. (28).

[1] T. Brabec and F. Krausz, Rev. Mod. Phys. **72**, 545 (2000).
[2] E. Gouliemakis *et al.*, Science **305**, 1267 (2004).
[3] G. G. Paulus, F. Grasbon, H. Walther, P. Villoresi, M. Nisoli, S. Stagira, E. Priori, and S. De Silvestri, Nature (London) **414**, 182 (2001).
[4] D. B. Milosević, G. G. Paulus, D. Bauer, and W. Becker, J. Phys. B **39**, R203 (2006).
[5] S. Geltman, J. Phys. B **33**, 1967 (2000).
[6] J. P. Hansen, J. Lu, L. B. Madsen, and H. M. Nilsen, Phys. Rev. A **64**, 033418 (2001).
[7] X. M. Tong, Z. X. Zhao, and C. D. Lin, J. Phys. B **36**, 1121 (2003).
[8] D. Dimitrovski and E. A. Solov'ev, J. Phys. B **39**, 895 (2006).
[9] L. V. Keldysh, Zh. Eksp. Teor. Fiz. **47**, 1945 (1964) [Sov. Phys. JETP **20**, 1307 (1965)].
[10] F. H. M. Faisal, J. Phys. B **6**, L89 (1973); H. R. Reiss, Phys. Rev. A **22**, 1786 (1980).
[11] Yu. N. Demkov and V. N. Ostrovskii, *Zero Range Potentials and their Application in Atomic Physics* (Plenum Press, New York, 1988).
[12] N. L. Manakov, M. V. Frolov, B. Borca, and A. F. Starace, J. Phys. B **36**, R49 (2003).
[13] W. Becker, S. Long, and J. K. McIver, Phys. Rev. A **50**, 1540 (1994).
[14] D. Dimitrovski, Ph.D. thesis, University of Freiburg, 2005 (unpublished) (available online at Die Deutsche Bibliothek, online at http://deposit.ddb.de/cgi-bin/dokserv?idn=975998935).
[15] D. Dimitrovski, T. P. Grozdanov, E. A. Solov'ev, and J. S. Briggs, J. Phys. B **36**, 1351 (2003).
[16] L. D. Landau and E. M. Lifshitz, *Quantum Mechanics: Non-Relativistic Theory* (Pergamon Press, Oxford, 1962).
[17] B. A. Lippmann and T. F. O'Malley, Phys. Rev. A **2**, 2115 (1970).
[18] A. I. Greiser, Sov. Phys. J. **17**, 1225 (1974).
[19] Yu. N. Demkov and G. F. Drukarev, Zh. Eksp. Teor. Fiz. **47**, 918 (1964) [Sov. Phys. JETP **20**, 614 (1965)].
[20] B. Gottlieb, M. Kleber, and J. Krause, Z. Phys. A **339**, 201 (1991).
[21] S. X. Hu and A. F. Starace, Phys. Rev. A **68**, 043407 (2003).
[22] G. F. Gribakin and M. Yu. Kuchiev, Phys. Rev. A **55**, 3760 (1997).
[23] O. Smirnova, M. Spanner, and M. Ivanov, J. Phys. B **39**, S307 (2006).
[24] D. Bauer and P. Mulser, Phys. Rev. A **59**, 569 (1999).
[25] V. P. Krainov, J. Opt. Soc. Am. B **14**, 425 (1997).
[26] A. Scrinzi, M. Geissler, and T. Brabec, Phys. Rev. Lett. **83**, 706 (1999).
[27] X. M. Tong and C. D. Lin, J. Phys. B **38**, 2593 (2005).
[28] J. S. Briggs, V. I. Savichev, and E. A. Solov'ev, J. Phys. B **33**, 3363 (2000).